Towards a global 3D upper mantle attenuation model using SEM

Jamie Barron[1], Vedran Lekić[2], Scott French[3] and Barbara Romanowicz[1,3]

1. Institut de Physique du Globe de Paris 2. Department of Geology, University of Maryland 3. Berkeley Seismological Laboratory, UC Berkeley

1. Summary

We present here the first results of a very preliminary inversion for *Q* structure, starting from a SEM-based global elastic model. These initial results recover some of the gross features of existing upper mantle *Q* models. Since we have not as yet applied corrections for source and receiver terms, nor employed sophisticated data selection techniques, nor applied crustal corrections, and have only used the fundamental Rayleigh wave mode in the inversions (i.e. we have not used horizontal components or overtone data), the recovery of these features shows promise for the future development of a SEM-based *Q* model, in conjunction with refinements to the existing elastic SEM-based model.

2. Motivation

Determining the global 3-D anelastic structure in the mantle is important step towards a better understanding of the dynamics and structure of the Earth. The quality factor *Q* is considerably more sensitive to temperature than elastic velocity, which implies that *Q* tomography can provide us with additional constraints on the thermal structure of the earth, complementing the information provided by elastic tomography, and possibly enabling us to distinguish the distribution of chemical versus thermal heterogeneity in the mantle. In addition, attenuation causes dispersion of seismic waves and this effect needs to be taken into account in constructing and interpreting seismic velocity models.

However, since inversion for *Q* exploits the amplitude information in the seismogram, we require the elastic structure to be well-modelled before we can extract the *Q* signal - i.e. good phase alignment. In addition, elastic effects such as focusing and defocusing affect the amplitude of the seismogram, and could potentially be mapped into *Q* if the elastic structure is not well-modelled, or alternatively if paths showing strong focusing and defocusing are not excluded. Previous *Q* models have required very careful data selection in their construction to avoid these effects. There are relatively few existing models, and there is not nearly the same level of agreement at long wavelength between *Q* models as there is between elastic velocity models.

The advent of SEM-based global elastic tomography (Lekic & Romanowicz, 2011; French et al. 2011) provides a new starting point for the resolution of *Q* structure in the upper mantle. These models take into account focussing and defocussing of elastic waves, through the use of the SEM for the forward modelling step. High amplitude slow anomalies are better recovered, and waveform fits are improved compared to previous models. This therefore provides an ideal starting point for a *Q* inversion, which can be further improved through more iterations of SEM modelling and further inversions for elastic and anelastic structure. Our preliminary model here recovers features seen in previous global *Q* inversions without yet having taken account of many corrections which we will implement in the inversion scheme in future development.

3. SEM elastic tomography - our starting model for *Q* inversion

We use the SEMum2.2 mantle model (French et al., 2011) as the elastic starting model in our *Q* inversion, which is developed by additional iterations from SEMum of Lekic & Romanowicz (2011). The SEM-based global tomography uses the coupled spectral element method (cSEM) of Capdeville (2003) to forward model the wavefield for each event in the current model iteration. The use of accurate forward modelling captures the effects of focusing and defocusing, and this leads to improved amplitude recovery of elastic anomalies in the model, particularly low-velocity regions. The crust used in the forward simulation is a homogenized crust with a minimum thickness of 30km (a filtered version of the Crust2.0 Moho is used where the thickness is >30km).

The kernels used in the inversion are calculated using the non-linear asymptotic coupling method (NACT) of Li & Romanowicz (1995). This introduces an additional term to the path average approximation to account for coupling across normal mode dispersion branches, and the kernels capture finite-frequency effects in the vertical plane of the great-circle path. In the inversion, wavepackets are weighted according to their type and redundancy, which allows the fitting of overtone energy and equalizes sensitivity to horizontally and vertically polarized wavefields. This weighting means that if we were to do an adjoint inversion, separate kernels would have to be calculated for each wavepacket, which would be too computationally expensive. Crustal contamination is minimized by supplementing the waveform dataset with group velocity dispersion maps in the inversion step.

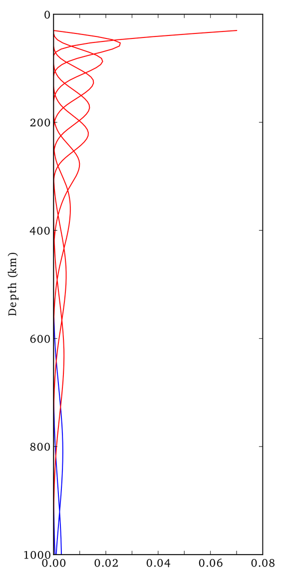

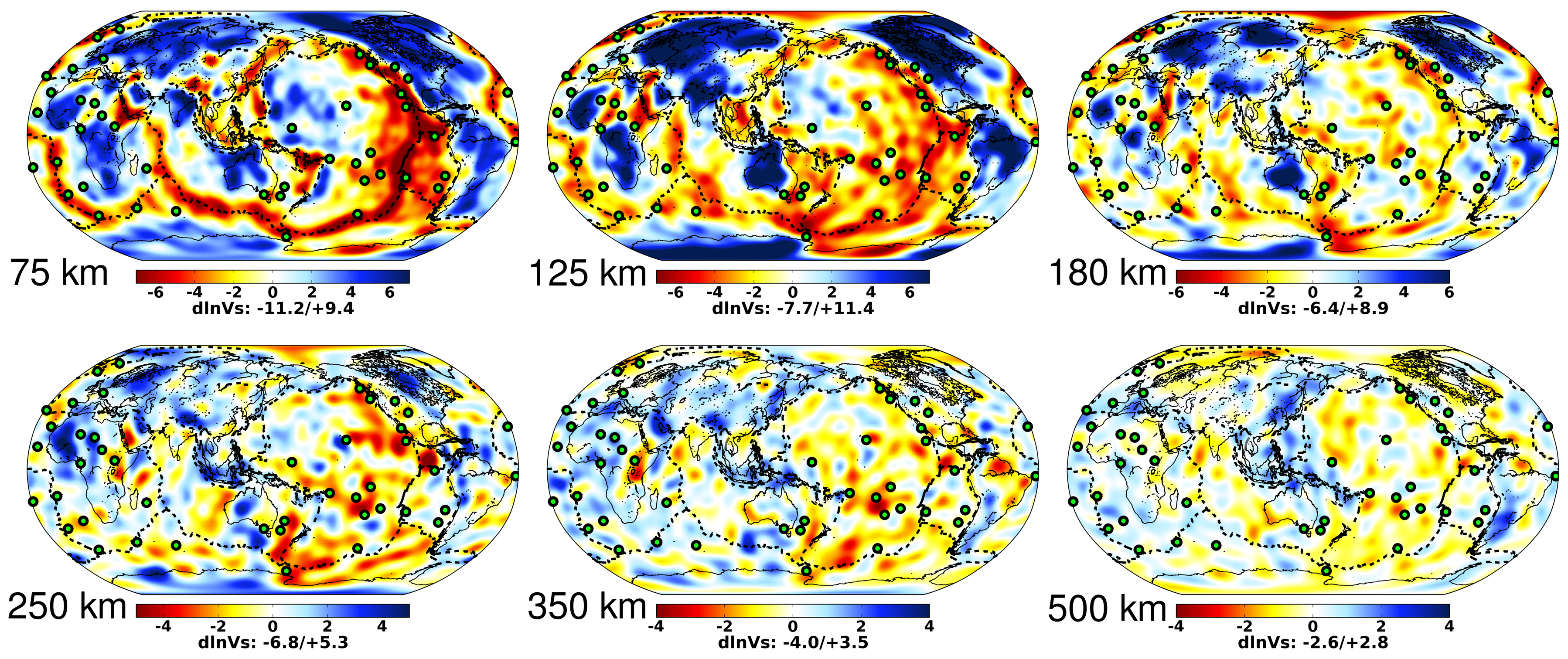

Figure 1: Model SEMum2.2 (French et al., 2011). Upper right: vertical B-spline knots used to parametrize the upper part of the model. Those marked in red are inverted for in the *Q* inversion.

4. Normal mode perturbation theory *Q* kernels

The calculation of the *Q* kernels (partial derivatives of the seismogram with respect to the *Q* model perturbation) used in the inversion is done using the NACT normal mode perturbation code (Li & Romanowicz, 1995), although currently only the path-average approximation is used, not the cross-branch coupling (which was used in the calculation of the elastic kernels, see panel 3). It was necessary to modify the code to include the anelastic effects. The figures below show tests verifying *Q* implementation in the modified code.

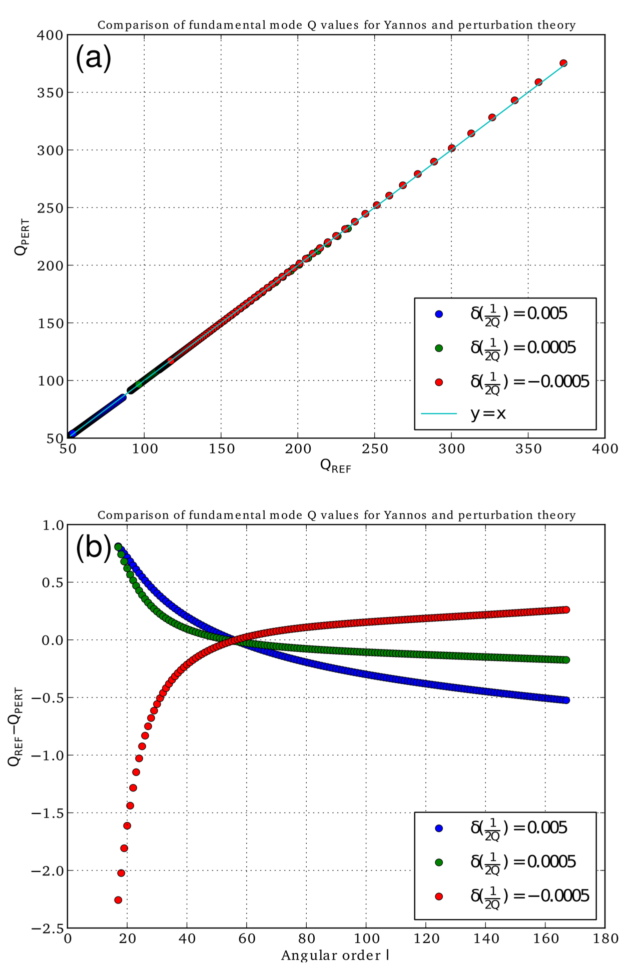

Figure 2 (left): Comparison of fundamental mode *Q* values obtained by forward modelling using a constant perturbation in the modified normal-mode perturbation code with those obtained by applying the same perturbation in the reference model and calculating *Q* for each mode directly. (a) shows the *Q* from perturbation theory plotted against *Q* from the direct calculation. (b) shows the difference between the perturbation theory *Q* and the direct calculation plotted as a function of angular order.

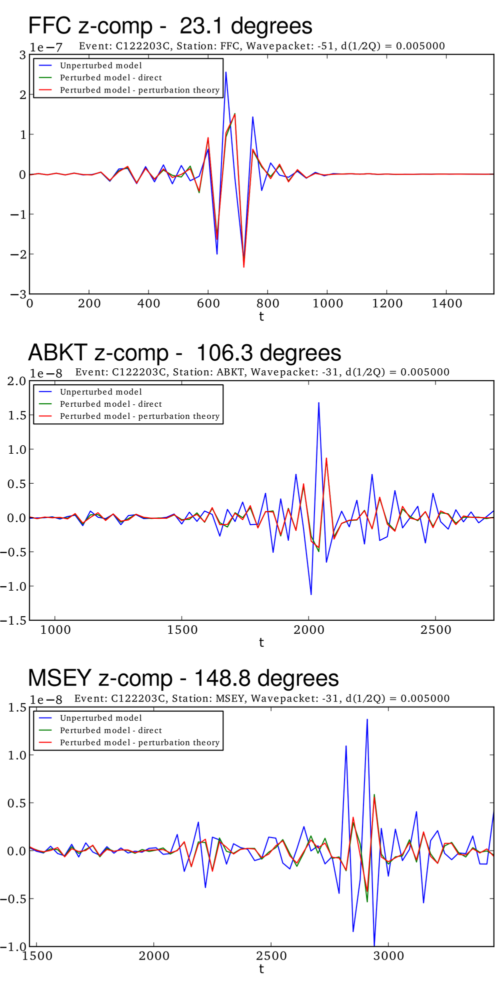

Figure 3 (right): Comparison of seismograms calculated using perturbation theory and a constant *Q* perturbation (red line) with those calculated by changing the reference model by the same constant perturbation (green line). In all plots a constant perturbation to d(1/2*Q*) of +0.005 has been used. Agreement is good for all wavepackets over the range of epicentral distances shown. The reference model is PREM with *Q* from QL6 (calculation in the original reference model is shown with a blue line).

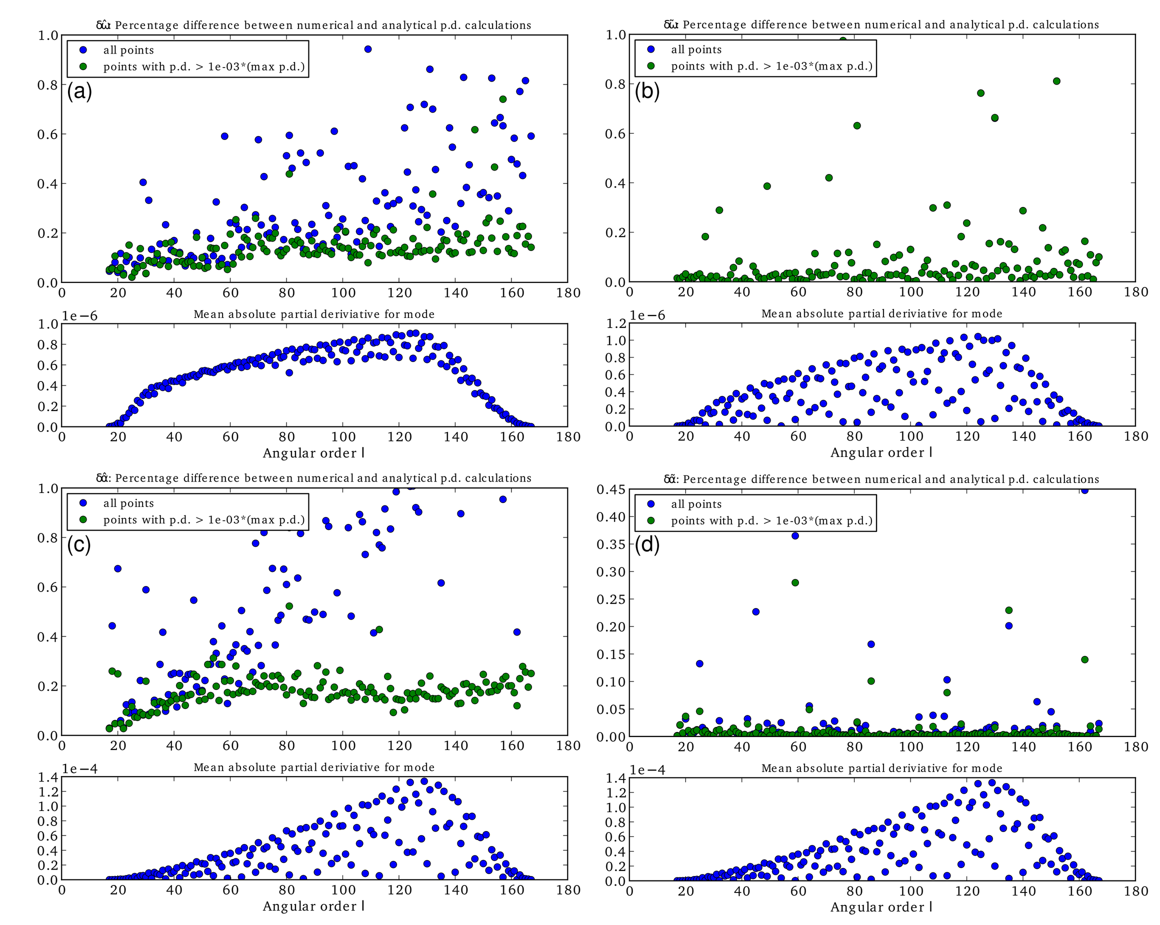

Figure 4 (left): Verification of the terms for the partial derivative of the seismogram with respect to the great-circle (^) and minor arc (~) average of angular frequency shift(δω) and imaginary angular frequency shift corresponding to the *Q* effect (δα). Each term is compared against the same derivative computed numerically for a perturbation of 1% in the quantity. Agreement is good except in cases where the derivative is small compared to the maximum for the mode, or the mean partial derivative for that mode itself is small, indicating that any errors are likely to be numerical, and in any case will not affect the inverse problem.

5. Preliminary *Q* Model

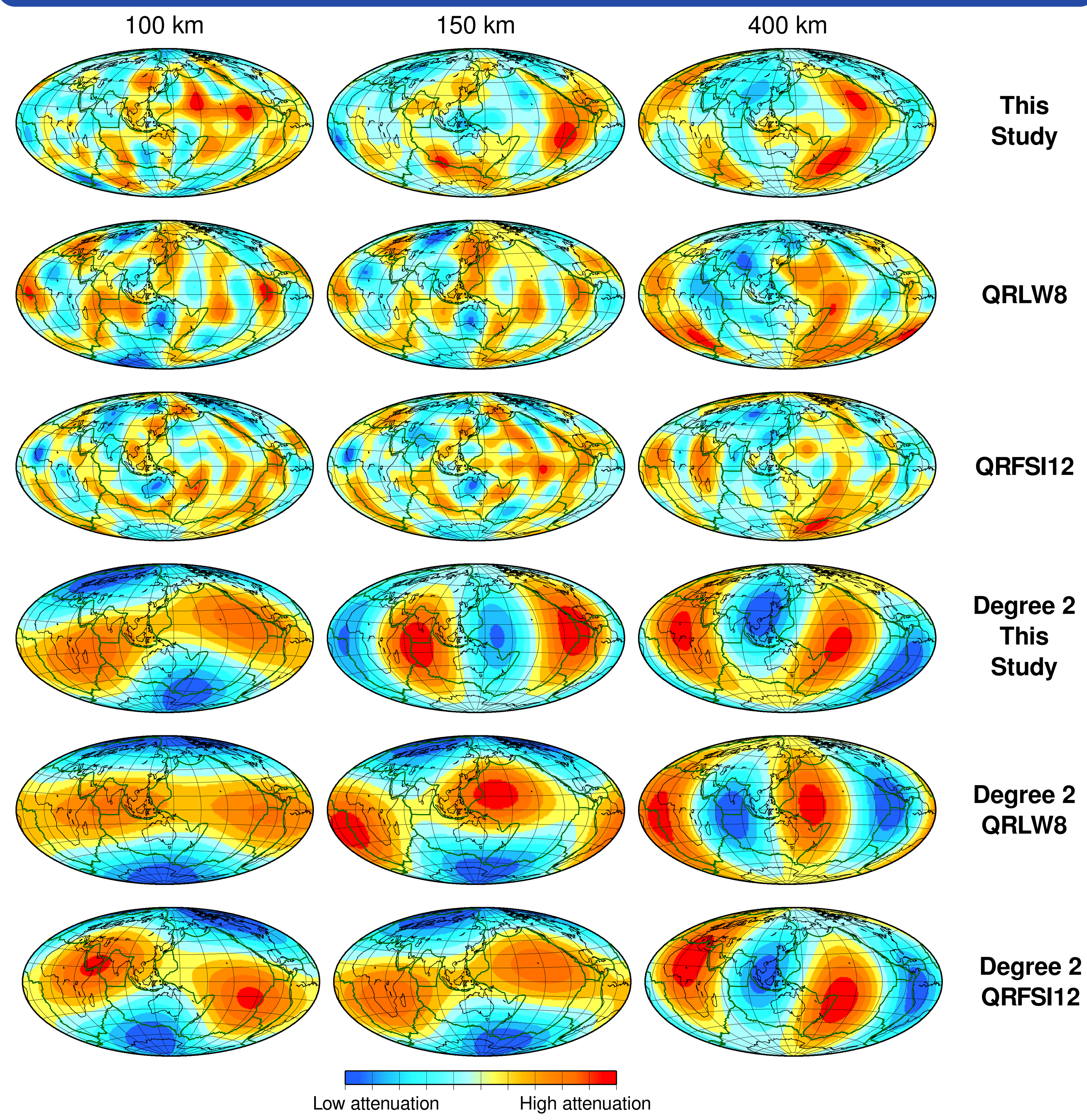

Figure 5 (above): Very preliminary, first iteration, *Q* model based on the inversion of SEM synthetics from the last iteration of SEMum2.2, compared to existing *Q* models QRLW8 (Gung & Romanowicz, 2004) and QRFSI12 (Dalton et al., 2008). The top three rows show the complete models and the bottom three the spherical harmonic degree 2 component of the models. Our model is based only on the inversion of fundamental mode Rayleigh wavepackets (minor and major arc), and as yet features no crustal corrections nor source and receiver term corrections. Wavepackets have been used in the inversion if the correlation coefficient between the SEM synthetic and the data is greater than 0.5: we used 10,318 wavepackets for the 199 events. The model has been inverted with a horizontal correlation length of 5000km and a vertical correlation length of 100km.

While this is still a very preliminary model, and neglects many correction terms that will be included in our future work, we are nevertheless recovering upper mantle attenuation features that have been seen in previous *Q* models, such as a correlation with tectonics in the upper 200km of the model (low attenuation in the cratons and high attenuation along ridges and in the back-arcs), and such as the degree 2 pattern beneath Africa and the Pacific seen at deeper depths.

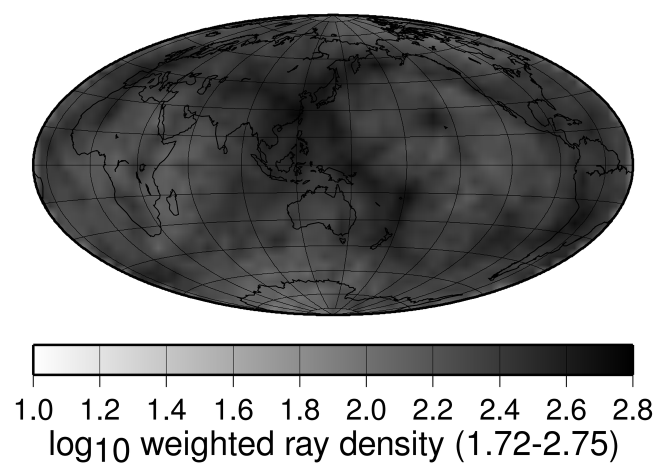

Figure 6 (right): Log-weighted (based on the wavepacket weights applied in the inversion) data coverage for our Q model.

References

Capdeville, Y., Chaljub, E., Vilotte, J.-P. & Montagner, J.-P., 2003. Coupling the spectral element method with a modal solution for elastic wave propagation in global earth models, *Geophys J. Int.*, **152**, 34–67.
Dalton, C. A., Ekström, G. & Dziewoński, A. M., 2008. The global attenuation structure of the upper mantle, *J. Geophys. Res.*, **113**, B09303.
French, S. W., Lekić, V., & Romanowicz, B., 2011. Toward global waveform tomography with the SEM: Improving upper-mantle images, Abstract S13C-02 presented at 2011 Fall Meeting, AGU, San Francisco, USA, 5-9 Dec.
Gung, Y. & Romanowicz, B., 2004. Q tomography of the upper mantle using three-component long period waveforms, *Geophys. J. Int.*, **157**, 813–830.
Lekić, V. & Romanowicz, B., 2011. Inferring upper-mantle structure by full waveform tomography with the spectral element method, *Geophys. J. Int.*, **185**: 799–831.
Li, X.-D. & Romanowicz, B., 1995. Comparison of global waveform inversions with and without considering cross-branch modal coupling, *Geophys J. Int.*, **121**, 695–709

Contact: barron@ipgp.fr Institut de Physique du Globe de Paris, 1 rue Jussieu, Paris, 75005 France http://www.ipgp.fr